

See discussions, stats, and author profiles for this publication at: <https://www.researchgate.net/publication/267742494>

Non-wettable, Oxidation-Stable, Brightly Luminescent, Perfluorodecyl-Capped Silicon Nanocrystal Film

ARTICLE in JOURNAL OF THE AMERICAN CHEMICAL SOCIETY · OCTOBER 2014

Impact Factor: 12.11 · DOI: 10.1021/ja5081037 · Source: PubMed

CITATION

1

READS

100

13 AUTHORS, INCLUDING:



Chenxi Qian

University of Toronto

6 PUBLICATIONS 7 CITATIONS

SEE PROFILE



Jia Jia

University of Toronto

3 PUBLICATIONS 2 CITATIONS

SEE PROFILE



Benjamin Hatton

University of Toronto

51 PUBLICATIONS 2,123 CITATIONS

SEE PROFILE



Gilberto Casillas

University of Wollongong

55 PUBLICATIONS 427 CITATIONS

SEE PROFILE

Non-wettable, Oxidation-Stable, Brightly Luminescent, Perfluorodecyl-Capped Silicon Nanocrystal Film

Chenxi Qian,[†] Wei Sun,[†] Liwei Wang,^{†,‡} Changlong Chen,^{†,§} Kristine Liao,[†] Wendong Wang,^{||} Jia Jia,^{†,⊥} Benjamin D. Hatton,[⊥] Gilberto Casillas,[#] Marty Kurylowicz,[▽] Christopher M. Yip,[▽] Melanie L. Mastronardi,[†] and Geoffrey A. Ozin^{*,†}

[†]Department of Chemistry, University of Toronto, Toronto, Ontario M5S 3H6, Canada

[‡]Tianjin Key Lab of Metal and Molecule-based Material Chemistry, Department of Chemistry, Nankai University, Tianjin 300071, P. R. China

[§]School of Chemistry and Chemical Engineering, University of Jinan, Jinan, Shandong 250022, P. R. China

^{||}Wyss Institute for Biologically Inspired Engineering, and School of Engineering and Applied Sciences, Harvard University, Cambridge, Massachusetts 02138, United States

[⊥]Department of Materials Science & Engineering, University of Toronto, Toronto, Ontario M5S 3E4, Canada

[#]Electron Microscopy Centre, University of Wollongong, New South Wales 2500, Australia

[▽]Department of Biochemistry, and Terrence Donnelly Centre for Cellular and Biomolecular Research, University of Toronto, Toronto, Ontario M5S 3H6, Canada

Supporting Information

ABSTRACT: Here we describe for the first time the synthesis of colloidally stable, brightly luminescent perfluorodecyl-capped silicon nanocrystals and compare the properties of solutions and films made from them with those of their perhydrodecyl-capped relatives. The perfluorodecyl capping group compared to the perhydrodecyl capping group yields superior hydrophobicity and much greater resistance to air oxidation, the enhanced electron-withdrawing character induces blue shifts in the wavelength of photoluminescence, and the lower-frequency carbon–fluorine stretching modes disfavor non-radiative relaxation pathways and boost the absolute photoluminescence quantum yield. Together these attributes bode well for advanced materials and biomedical applications founded upon perfluorodecyl-protected silicon nanocrystals.

The burgeoning research activity on new kinds of nanostructured silicon, made from one of the most abundant and green materials on earth, is striking.^{1,2} This activity transcends the utilization of top-down nanofabricated silicon for integration in the incredible shrinking world of more powerful and faster microelectronics. What is remarkable is the notable intensification of research on bottom-up synthesized forms of nanostructured silicon for everything other than microelectronics.^{3–6} Moreover, the purported non-toxicity⁷ and biocompatibility^{8,9} of nanometer-scale silicon allows it to be marketed as a “green” material in the emerging field of medical theranostics. One can easily find a long list highlighting prominent reports on nanometer-scale silicon in the recent literature. The typical synthesis involves a hydrosilylation reaction, which enhances the solution-processability of the material. This is also an important route in the field of silicon

surface chemistry, exemplified by the pioneering work of Buriak, Veinot, Kortshagen, Swihart, etc.^{10–14}

However, the instability against oxidation has been a major drawback for nanostructured silicon in various applications. There are situations where silicon nanostructured materials could benefit from water resistance, and this can, in principle, be achieved by protecting the surface with super-hydrophobic molecules or polymers, the best documented examples being based on perfluorohydrocarbons. Specifically, we aim to avoid or ameliorate the situations when silicon nanocrystals are exposed in air and the ambient water accelerates the oxidation of the silicon core, thereby decreasing the photoluminescence quantum yield^{15,16} significantly. The phenomenon of non-wettability stems from the extremely low polarizability of fluorine and the very strong carbon–fluorine single bond, which causes very weak van der Waals interactions with perfluorohydrocarbons. While fluoro-substituted alkenes have been chemically anchored to the surface of silicon wafers and porous silicon,¹⁷ freestanding perfluorodecyl-capped silicon nanocrystals have never been reported before.

In this context, it is interesting to contemplate the effect of covalently grafting perfluoroalkane groups to the surface of silicon nanocrystals rather than the perhydroalkanes that have been exclusively reported^{17–21} to date. How would this affect their colloidal stability and wettability, their electronic and optical properties, and their stability against oxidation? In this Communication we describe for the first time the synthesis and characterization of freestanding perfluorodecyl-capped silicon nanocrystals and measure, compare, and discuss the aforementioned behaviors in relation to those of the perhydroalkane analogue. From the point of view of designing and synthesizing solid-state materials, it is a demonstration of controlling

Received: August 7, 2014

Published: October 27, 2014



surface-property relations—how the surface correlates to and affects the stability of the nanomaterial under certain conditions.

Our synthesis was performed using a microwave reactor, in a closed vial. It is important to note that this reaction system uniquely guarantees a typical hydrosilylation temperature of 170 °C, which is higher than the boiling point of the solvent, 1*H*,1*H*,2*H*-perfluoro-1-decene. The upper layer was decane and the lower was 1*H*,1*H*,2*H*-perfluoro-1-decene since they were not miscible. The reaction proceeded for 3 h to achieve sufficient surface coverage.²² In order to get an even higher surface ligand density and better colloidal stability, we extended the reaction time to 24 h. Before the reaction, the hydride-terminated silicon nanocrystals were dispersed in the upper layer of decane; after the reaction, they descended to the lower layer of 1*H*,1*H*,2*H*-perfluoro-1-decene (Figures 1 and S1). It

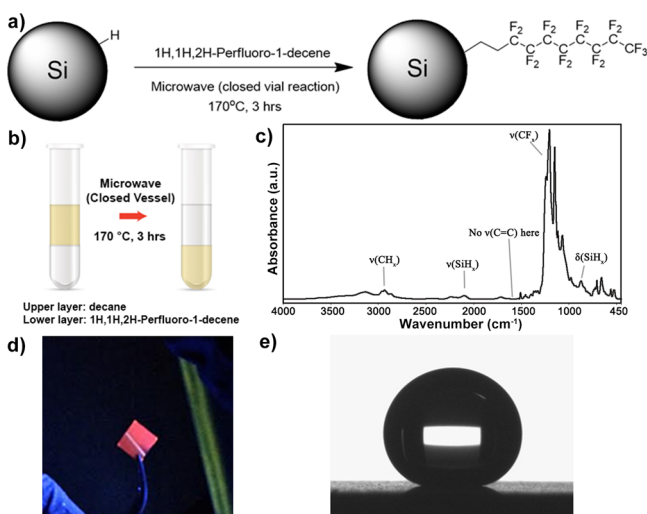


Figure 1. (a,b) Schematic illustration of the synthesis of perfluorodecyl-capped silicon nanocrystals (ncSi:PFD). (c) FT-IR spectrum of ncSi:PFD. (d) Photoluminescence shown by the spin-coated ncSi:PFD film on a silicon wafer. (e) Image of a water droplet sitting on the super-hydrophobic film composed of ncSi:PFD.

was observed that, at 170 °C, the two solvents were miscible. So the hydrosilylation process was actually a homogeneous reaction. The dispersion of the product by an overnight reaction was still colloidally stable after 1 month. After the hydrosilylation, the surface of the silicon nanocrystal was covalently bonded by tetrahydro-perfluorocarbon chains, which was confirmed by Fourier transform infrared (FTIR) spectroscopy (Figure 1c) and X-ray photoelectron spectroscopy (XPS) (Figure S3). The perfluorodecyl-capped silicon nanocrystals (ncSi:PFD) were 3–5 nm in diameter, which is supported by the HR-STEM images (Figure S4) and atomic force microscopy (AFM) data (Figure S8).

We spin-coated the ncSi:PFD onto a single-crystal silicon wafer surface. The wafer surface was pretreated²³ with 1*H*,1*H*,2*H*,2*H*-perfluorooctylsilane (PFOTS) to facilitate the anchoring of the perfluorocarbon-capped silicon nanocrystals (Figure S2). Through this method, we obtained uniform films with almost full surface coverage by the ncSi:PFD. A hierarchical structure of the film can be seen through the SEM and AFM images (Figures S5 and S8). The ncSi:PFD film showed bright photoluminescence (PL) (Figures 1d and 2b). The surface of the film as prepared was already super-

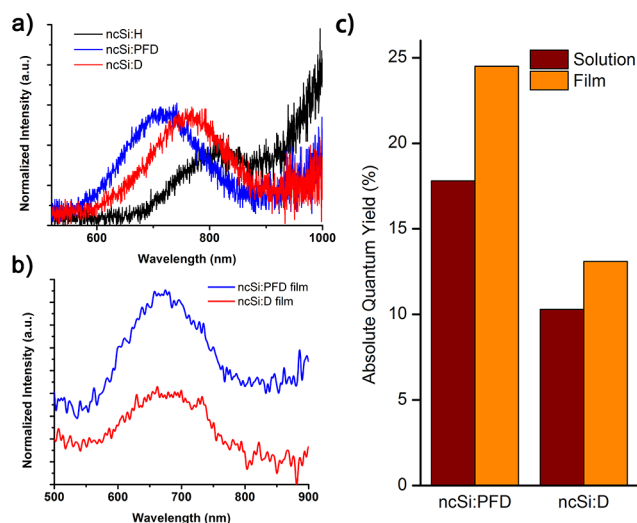


Figure 2. (a) Photoluminescence spectra of hydride-, decyl-, and perfluorodecyl-capped silicon nanocrystals in solution. (b) Photoluminescence spectra of decyl- and perfluorodecyl-capped silicon nanocrystals in the solid state (film). (c) Comparison between the absolute quantum yield of decyl- and perfluorodecyl-capped silicon nanocrystals in solution and in the solid state.

hydrophobic after the facile step of spin-coating, without any further treatment (Figure 1e). Water droplets roll off the surface easily (Supporting Information, movies). This surface shows a water contact angle (CA) of $168.3 \pm 0.5^\circ$. The advancing and receding CAs of the surface are 167.7° and 168.8° , respectively (Figure S7). AFM showed that the film had different root-mean-square roughness at different length scales (Figure S8). The interplay of the multiscale hierarchical structure and low surface free energy contributes to the super-hydrophobicity. The multiscale roughness and the cavities suggest the existence of a Cassie–Baxter^{24,25} surface state. A very low sliding angle is also evidence of such a state. A control experiment showed that a PFOTS-treated silicon wafer surface did not exhibit an ultra-water-repellent character, with a water CA measured at around 117° . Another control experiment was done with a film composed of decyl-group-capped silicon nanocrystals (ncSi:D), which showed no super-hydrophobicity either (Figure S6). This comparison confirms that the super-hydrophobic nature is from the ncSi:PFD film itself and the constituent nanocrystals.

The ncSi:PFD dispersion was brightly photoluminescent, and the spectra shifted to the blue compared to the spectra of ncSi:H and ncSi:D dispersions (Figure 2a). The emission tails shown at above 900 nm were from the larger particles within the ensemble.⁶ The blue shift can be explained by the lack of aggregation and less electronic coupling compared to ncSi:H dispersions. Due to the lower vibrational levels of ncSi:PFD, they possessed a slightly larger gap, and the corresponding spectra shifted further toward the shorter wavelength. The PL spectra of ncSi:PFD and ncSi:D films are shown in Figure 2b. Free from non-radiative solvent relaxations and relaxations via intramolecular rotation, both the ncSi:PFD and ncSi:D films had a higher absolute quantum yield (AQY) than the nanocrystal dispersions (Figure 2c).

A few factors contribute to the higher AQY of ncSi:PFD (dispersion or film) compared with ncSi:D (dispersion or film). First, the lower frequency carbon–fluorine stretching mode disfavors non-radiative relaxation pathways and boosts the

absolute photoluminescence quantum yield.^{26,27} Specifically, there is less coupling between lower vibrational levels and the electronic excited states; thus, fewer internal conversions occur and non-radiative relaxations are rarer. Second, ncSi:PFD are more stable against oxidation and have fewer oxidation defects (see below). Previous reports²⁸ have shown that the introduction of surface oxidation defects would affect the optical properties of silicon nanocrystals and reduce the photoluminescence quantum yield significantly.

Since the as-synthesized perfluorodecyl-capped silicon nanocrystals still had remnant terminal hydrides (which was confirmed by FTIR, Figure 1c), they could easily undergo oxidation to hydroxide and oxide in the presence of ambient oxygen and water. It is well-recognized that the oxidation of silicon nanocrystals usually follows the Cabrera–Mott mechanism,^{29,30} as supported by previous investigations.^{31–33} This mechanism describes how a Si crystal surface is oxidized by the simultaneous presence of water and oxygen molecules in the ambient air. Specifically, the polar water molecules approach the surface silanol groups preferentially and aid in the cleavage of Si–Si bonds adjacent to the silanol groups. Then an electron is transferred from the broken bond to an adsorbed oxygen molecule. So it can be speculated that the presence of ambient water accelerates the oxidation process, and a water-repellent perfluorodecane surface, on the other hand, can contribute to slowing down such a process.

In order to confirm the expected difference between the ncSi:D and ncSi:PFD films in reactivity, we compared the oxidation trends of the two films (ncSi:D and ncSi:PFD) over a period of time by FTIR. Both films were prepared freshly from the same batch of ncSi:H and were exposed to air under the same ambient conditions (25% relative humidity (RH)). We investigated the same regions of the FTIR spectra of the ncSi:D and ncSi:PFD, as shown in Figure 3a,b, respectively. The Si–O–Si mode is centered at 1070 cm^{−1}. The absolute difference in absorption around this region reflects the extent of oxidation. Since the films were prepared freshly at zero hour when little oxidation occurred, a distinct comparison between the peak heights in Figure 3a,b would be a fair comparison of the extent of oxidation. As expected, the result indicates that under the same ambient conditions, the ncSi:D film was oxidized much faster than the ncSi:PFD film was. We also investigated the oxidation of both films exposed to the same humid air (94% RH) and compared their reactivity, in which case the ncSi:D film was also oxidized much faster than the ncSi:PFD film, again as expected (Figure 3c,d). It was observed that in a highly humid environment the ncSi:PFD film was still resistant to oxidation.

On the other hand, it is important to further investigate the stability of the films by measuring the AQY after different times of exposure in air with different ambient RH. Figure S9a shows the evolution of the AQY under different conditions of the film samples made of ncSi:PFD/ncSi:D prepared with a reaction time of 24 h. The AQY of the ncSi:D film after exposure to air (68% RH) for 30 min dropped significantly, while that of the ncSi:PFD film dropped relatively less. The case was similar with exposure to air (92% RH) for 15 h. The comparison of the relative drop in AQY is summarized in Figure 4 as pie charts. In ambient air with lower RH (25%), the relative AQY drop for both films was much slower, measured at 3.92% for ncSi:PFD film and 13.01% for ncSi:D film after 8 days' exposure (absolute value shown in Figure S9b). This comparison (shown in Figure 4) corresponds well with the difference in oxidation rates

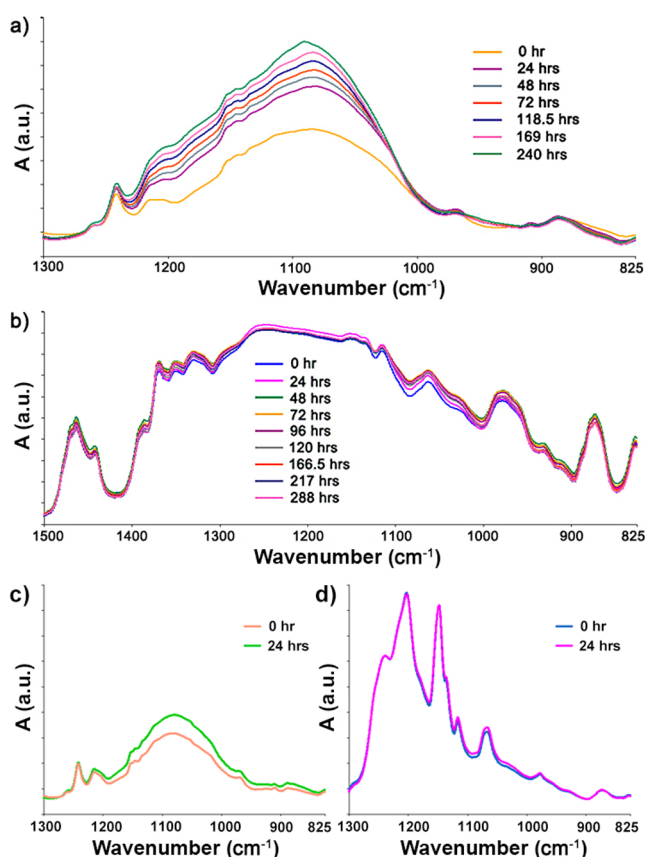


Figure 3. Oxidation trends of silicon nanocrystal films overtime: (a) ncSi:D film in ambient air, (b) ncSi:PFD film in ambient air, (c) ncSi:D film in humid air, and (d) ncSi:PFD film in humid air.

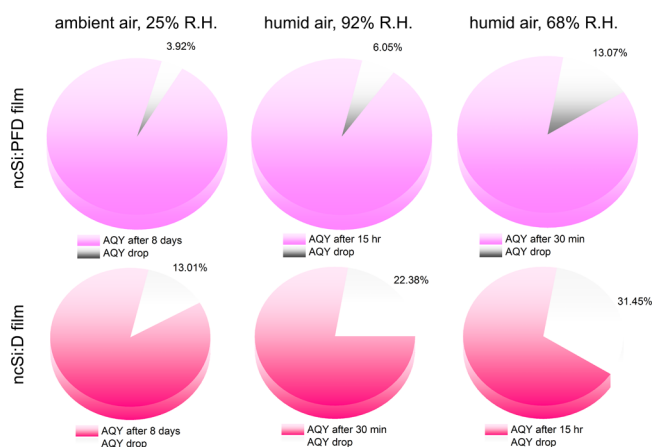


Figure 4. Comparison of the relative drop in absolute quantum yield (AQY) of two films under different conditions (area of the pies reflect the initial absolute values of AQY, 35% for ncSi:PFD film and 28% for ncSi:D film): top, ncSi:PFD film; bottom, ncSi:D film; left, exposed to air (25% RH) for 8 days; middle, exposed to air (92% RH) for 30 min; right, exposed to air (68% RH) for 15 h.

indicated by the FTIR mentioned above. Clearly, water assisted the oxidation but at the same time passivated the surface as a type of protection. These two competing effects could explain why, in extremely high RH, the oxidation was slower for both materials compared to those in humid air with moderate RH. A future thorough study is planned to obtain information about the detailed mechanism. We also observed a much faster

intensity drop of the ncSi:D film than the ncSi:PFD film after it was immersed in distilled water for hours (Figure S10). Clearly, it was undisputable that, in any case, the ncSi:PFD film was always more stable than the ncSi:D film in maintaining its photoluminescence AQY.

In summary, free-standing silicon nanocrystals capped by perfluoroalkane chains were synthesized, and a higher absolute quantum yield was obtained both for dispersions and films compared to those made from their perhydroalkane analogues. Films of these perfluoroalkane-capped silicon nanocrystals were proven to be super-hydrophobic and found to be much more resistant to air oxidation than the perhydroalkane analogue. It is a new, facile, and green way of fabricating bifunctional photoluminescent super-hydrophobic nanocrystal surfaces. Future work may include the synthesis of PEG-terminated solid lipid particles composed of these ncSi:PFD for better biocompatibility and biostability in biomedical applications.³⁴ Collectively these observations speak well for advanced materials and biomedical uses for these perfluoroalkane-capped silicon nanocrystals.

■ ASSOCIATED CONTENT

■ Supporting Information

Chemicals and materials, instruments, experimental details; characterizations including FTIR, HR-TEM, XPS, SEM, and AFM; and super-hydrophobicity comparisons between films made by perfluorodecane-capped silicon nanocrystals and the perhydroalkane analogue, including videos. This material is available free of charge via the Internet at <http://pubs.acs.org>.

■ AUTHOR INFORMATION

Corresponding Author

gozin@chem.utoronto.ca

Notes

The authors declare no competing financial interest.

■ ACKNOWLEDGMENTS

G.A.O. is Government of Canada Tier 1 Canada Research Chair in Materials Chemistry. The strong and sustained financial support of this research by the Natural Science and Engineering Research Council of Canada (NSERC) is deeply appreciated. A Premier Research Award in support of this research from the Ministry of Research Innovation (MRI) Ontario is also greatly acknowledged. C.Q. and W.S. are Connaught Scholars, and M.L.M. is a Vanier Graduate Scholar.

■ REFERENCES

- (1) Priolo, F.; Gregorkiewicz, T.; Galli, M.; Krauss, T. F. *Nanotechnol.* **2014**, *9*, 19.
- (2) Mastronardi, M. L.; Henderson, E. J.; Puzzo, D. P.; Ozin, G. A. *Adv. Mater.* **2012**, *24*, 5890.
- (3) Cheng, K.-Y.; Anthony, R.; Kortshagen, U. R.; Holmes, R. J. *Nano Lett.* **2010**, *10*, 1154.
- (4) Cheng, K.-Y.; Anthony, R.; Kortshagen, U. R.; Holmes, R. J. *Nano Lett.* **2011**, *11*, 1952.
- (5) Puzzo, D. P.; Henderson, E. J.; Helander, M. G.; Wang, Z. B.; Ozin, G. A.; Lu, Z. H. *Nano Lett.* **2011**, *11*, 1585.
- (6) Mastronardi, M. L.; Henderson, E. J.; Puzzo, D. P.; Chang, Y. L.; Wang, Z. B.; Helander, M. G.; Jeong, J. H.; Kherani, N. P.; Lu, Z. H.; Ozin, G. A. *Small* **2012**, *8*, 3647.
- (7) Alsharif, N. H.; Berger, C. E. M.; Varanasi, S. S.; Chao, Y.; Horrocks, B. R.; Datta, H. K. *Small* **2009**, *5*, 221.
- (8) Yang, Z.; Dasog, M.; Dobbie, A. R.; Lockwood, R.; Zhi, Y.; Meldrum, A.; Veinot, J. G. C. *Adv. Funct. Mater.* **2014**, *24*, 1345.
- (9) Liu, J.; Erogbogbo, F.; Yong, K.-T.; Ye, L.; Liu, J.; Hu, R.; Chen, H.; Hu, Y.; Yang, Y.; Yang, J.; Roy, I.; Karker, N. A.; Swihart, M. T.; Prasad, P. N. *ACS Nano* **2013**, *7*, 7303.
- (10) Buriak, J. M.; Stewart, M. P.; Geders, T. W.; Allen, M. J.; Choi, H. C.; Smith, J.; Raftery, D.; Canham, L. T. *J. Am. Chem. Soc.* **1999**, *121*, 11491.
- (11) Huck, L. A.; Buriak, J. M. *J. Am. Chem. Soc.* **2012**, *134*, 489.
- (12) Kelly, J. A.; Veinot, J. G. C. *ACS Nano* **2010**, *4*, 4645.
- (13) Mangolini, L.; Jurbergs, D.; Rogojina, E.; Kortshagen, U. *J. Lumin.* **2006**, *121*, 327.
- (14) Hua, F. J.; Swihart, M. T.; Ruckenstein, E. *Langmuir* **2005**, *21*, 6054.
- (15) Littau, K. A.; Szajowski, P. J.; Muller, A. J.; Kortan, A. R.; Brus, L. E. *J. Phys. Chem.* **1993**, *97*, 1224.
- (16) Wilcoxon, J. P.; Samara, G. A.; Provencio, P. N. *Phys. Rev. B* **1999**, *60*, 2704.
- (17) Stewart, M. P.; Buriak, J. M. *J. Am. Chem. Soc.* **2001**, *123*, 7821.
- (18) Mastronardi, M. L.; Hennrich, F.; Henderson, E. J.; Maier-Flaig, F.; Blum, C.; Reichenbach, J.; Lemmer, U.; Kubel, C.; Wang, D.; Kappes, M. M.; Ozin, G. A. *J. Am. Chem. Soc.* **2011**, *133*, 11928.
- (19) Kelly, J. A.; Shukaliak, A. M.; Fleischauer, M. D.; Veinot, J. G. C. *J. Am. Chem. Soc.* **2011**, *133*, 9564.
- (20) Yang, Z.; Iqbal, M.; Dobbie, A. R.; Veinot, J. G. C. *J. Am. Chem. Soc.* **2013**, *135*, 17595.
- (21) Buriak, J. M. *Chem. Mater.* **2014**, *26*, 763.
- (22) Sun, W.; Qian, C.; Mastronardi, M. L.; Wei, M.; Ozin, G. A. *Chem. Commun.* **2013**, *49*, 11361.
- (23) Sun, W.; Jia, F.; Sun, Z.; Zhang, J.; Li, Y.; Zhang, X.; Yang, B. *Langmuir* **2011**, *27*, 8018.
- (24) Cassie, A. B. D.; Baxter, S. *Trans. Faraday Soc.* **1944**, *40*, 0546.
- (25) Wang, S.; Jiang, L. *Adv. Mater.* **2007**, *19*, 3423.
- (26) Lin, S. H. *J. Chem. Phys.* **1966**, *44*, 3759.
- (27) Becker, R. S.; Pelliccioli, A. P.; Romani, A.; Favaro, G. *J. Am. Chem. Soc.* **1999**, *121*, 2104.
- (28) Pi, X. D.; Mangolini, L.; Campbell, S. A.; Kortshagen, U. *Phys. Rev. B* **2007**, *75*, 085423.
- (29) Mott, N. *Proc. R. Soc. A* **1981**, *376*, 207.
- (30) Cabrera, N.; Mott, N. F. *Rep. Prog. Phys.* **1948**, *12*, 163.
- (31) Pi, X. D.; Gresback, R.; Liptak, R. W.; Campbell, S. A.; Kortshagen, U. *Appl. Phys. Lett.* **2008**, *92*, 123102.
- (32) Liptak, R. W.; Kortshagen, U.; Campbell, S. A. *J. Appl. Phys.* **2009**, *106*, 064313.
- (33) Pereira, R. N.; Rowe, D. J.; Anthony, R. J.; Kortshagen, U. *Phys. Rev. B* **2011**, *83*, 155327.
- (34) Henderson, E. J.; Shuhendler, A. J.; Prasad, P.; Baumann, V.; Maier-Flaig, F.; Faulkner, D. O.; Lemmer, U.; Wu, X. Y.; Ozin, G. A. *Small* **2011**, *7*, 2507.